Astron. Astrophys. 345, 629–634 (1999)

ASTRONOMY
AND
ASTROPHYSICS

Abundance gradients in the outer galactic disk from planetary nebulae⋆

W.J. Maciel and C. Quireza

Instituto Astronômico e Geofísico, Universidade de São Paulo, Av. Miguel Stefano 4200, 04301-904 São Paulo SP, Brazil (maciel@iagusp.usp.br)

Received 1 December 1998 / Accepted 1 March 1999

Abstract. Radial abundance gradients of the element ratios O/H, Ne/H, S/H, and Ar/H are determined on the basis of a sample of disk planetary nebulae. The behaviour of the gradients at large distances from the galactic centre, $R > R_0 = 7.6$ kpc, is emphasized. It is concluded that the derived gradients are consistent with an approximately constant slope in the inner parts of the Galaxy, and some flattening for distances larger than R_0. A comparison is made with previous determinations using both photoionized nebulae and young stars, and some consequences on theoretical models for the chemical evolution of the galactic disk are discussed.

Key words: ISM: abundances – ISM: planetary nebulae: general – Galaxy: abundances

1. Introduction

The existence of radial abundance gradients is now firmly established, both in the galactic disk and also in the disks of other spiral galaxies. These gradients can be derived for several abundance ratios such as O/H and S/H, and can be determined from photoionized nebulae (HII regions and planetary nebulae) and young stars. Some references on abundance gradients in the Galaxy include: Shaver et al. (1983), Simpson et al. (1995), Vílchez & Esteban (1996), Rudolph et al. (1997) and Afflerbach et al. (1997) for HII regions; Fitzsimmons et al. (1990), Rolleston et al. (1993), Kaufer et al. (1994), Kilian-Montenbruck et al. (1994) and Smartt & Rolleston (1997) for young stars. For other spiral galaxies, see for example Villa-Costas & Edmunds (1992), Zaritsky et al. (1994), Henry & Howard (1995), Kennicutt & Garnett (1996), and Ferguson et al. (1998). A recent review on this subject is given by Maciel (1997).

The obtained results show a general agreement, especially regarding photoionized nebulae. The inclusion of stellar data introduces some degree of uncertainty, as these objects sometimes present shallower gradients than the photoionized nebulae. The situation is far from clear, however, and it may be possible that the gradients are relatively steeper in the inner portions of the Galaxy, at galactocentric distances lower than the sun's position, with some flattening near the outskirts of the galactic disk. Some references on this particular point include Vílchez et al. (1988), Henry & Howard (1995), Vílchez & Esteban (1996), Smartt & Rolleston (1997), and Ferguson et al. (1998).

The behaviour of the gradients has some important consequences regarding the models of chemical evolution, as some of these models predict an essentially constant gradient, while others are consistent with some change of slope for larger galactocentric distances and for objects of different ages (see for example Mollá & Ferrini 1995, Mollá et al. 1997, Chiappini et al. 1997, Samland et al. 1997, and Allen et al. 1998). It is therefore interesting to investigate not only the *magnitude* of the gradients, but also their *spatial* and *temporal* variations in the galactic disk.

Planetary nebulae (PN) play a distinct role in the solution of these problems, especially regarding the spatial and time variations of the gradients (D'Odorico et al. 1976, Faúndez-Abans and Maciel 1986, Peimbert 1990, Köppen et al. 1991, Maciel 1992, Samland et al. 1992, Pasquali & Perinotto 1993, Amnuel 1993, Maciel & Köppen 1994, Maciel & Chiappini 1994, and Peimbert & Carigi 1998). Previous work has shown that disk objects of type II are particularly useful in this respect (Faúndez-Abans & Maciel 1986, Maciel & Köppen 1994, Maciel & Chiappini 1994). Recently, Costa et al. (1997) studied a sample of galactic PN near the anticentre direction, obtaining new abundances for several objects which are probably located at distances greater than about 3 kpc from the sun, thus allowing a better determination of the gradients at large galactocentric distances.

In the present work, we consider the PN sample studied by Maciel & Köppen (1994) and Maciel & Chiappini (1994), plus the new objects by Costa et al. (1997) and redetermine the abundance gradients of O/H, Ne/H, S/H and Ar/H. Additionally, several objects selected from the Strasbourg-ESO Catalogue of Galactic Planetary Nebulae (Acker et al. 1992) and not included in the previous samples are also taken into account. In order to obtain a reliable classification, we have analysed several properties of the nebulae, comprising their chemical composition, morphology, space distribution and kinematical properties, as discussed for example by Maciel & Dutra (1992). As a consequence, our new sample forms the largest database of galactic

Send offprint requests to: W.J. Maciel

⋆ Table 1 is available only electronically at the CDS(anonymous ftp 130.79.128.5 or http://cdsweb.u-strasbg.fr/Abstract.html)

PN ever to be considered to estimate radial abundance gradients, for which all of those characteristics have been individually examined. Our main purpose is to study the presence of any slope variations along the galactic disk, especially at large galactocentric distances.

2. The data

The present investigation is based on a sample of galactic planetary nebulae generally classified as Type II objects, according to the classification scheme originally proposed by Peimbert (1978). As discussed elsewhere (Maciel 1992, Maciel and Köppen 1994), these nebulae closely reflect the properties of the interstellar medium out of which their central stars have been formed, particularly regarding the chemical elements that are not contaminated by the evolution of intermediate mass stars, such as oxygen, neon, sulphur and argon. Additionally, some objects have been included that have alternately been classified either as Type I or Type IIa PN, following the suggestion by Faúndez-Abans & Maciel (1987). In fact, the original criteria as proposed by Peimbert (1978) and Peimbert & Torres-Peimbert (1983) consider as Type I all nebulae having abundance ratios He/H > 0.125 or $\log$ (N/O) > -0.30. Recent work has shown that element enrichment in these objects is not uniform, suggesting a continuous enhancement which is probably related to the mass of the progenitor star (Cazetta & Maciel 1994, Maciel & Cazetta 1997). Therefore, a probably more correct approach would be to consider as Type I only those objects for which both conditions are satisfied. It would then be assured that these are the nebulae associated with the massive central stars which are closer to the high end of the mass interval $1 \leq M(M_\odot) \leq 8$ that characterizes the intermediate mass stars. As a consequence, objects for which only one of these conditions is satisfied would be considered as Type IIa (Faúndez-Abans & Maciel 1987), so that they are in fact Type II objects.

A basic sample of Type II nebulae was established by Maciel & Köppen (1994) and Maciel & Chiappini (1994), which forms the main body of the present investigation. This sample has been updated and extended after a search for PN probably located in the outskirts of the Galaxy in the Strasbourg-ESO Catalogue of Galactic Planetary Nebulae (Acker et al. 1992). Objects have been included for which new abundances have been determined by Costa et al. (1996, 1997), Corradi et al. (1997), Hajian et al. (1997), Kingsburgh & Barlow (1994), Perinotto et al. (1994), Perinotto (1991) and Köppen et al. (1991).

The sample has a total of 130 objects, which corresponds to an increase of about 40% relative to the earlier work of Maciel & Köppen (1994), which included 91 PN classified as Type II. Twenty of the added objects are new PN, and 19 have been reclassified as Type II. It is estimated that the average uncertainties of the abundances are $\sigma \simeq 0.1$ dex (cf. Maciel 1992, Maciel & Köppen 1994). The complete sample is given in Table 1[1], which is accessible in electronic form. The table lists for each object the common name, the PNG number (Acker et al. 1992), the adopted distance (kpc), the galactocentric distance (kpc), and the O, Ne, S, and Ar abundances, given as $\epsilon(\mathrm{X}) = \log(\mathrm{X/H}) + 12$, as usual. The last column lists the individual abundance references. In view of our comments at the end of Sect. 1, and of the fact that the new sample has been considerably increased, we expect that more reliable results can be derived from the present sample relative to previous work on radial gradients, particularly at galactocentric distances greater than the solar value.

The main source for the distances is the catalogue by Maciel (1984), supplemented by some individual distances from Cahn et al. (1992) and Amnuel et al. (1984). Although distances to PN are notoriously uncertain (cf. Terzian 1993, 1997), it has already been shown that these uncertainties tend to wash out any existing gradient, so that their main effect is to increase the observed scatter in the data (cf. Maciel & Köppen 1994, Maciel 1997).

Most of the recent work on galactic abundance gradients use the IAU recommended galactocentric distance at the sun's position, $R_0 = 8.5$ kpc. However, recent work based on the space distribution of globular clusters as well as other evidences suggest a somewhat lower distance, which may affect the determination of the gradients and especially their space variations. Therefore, in this work we have adopted the value recently derived from globular cluster analysis by Maciel (1993), $R_0 = 7.6 \pm 0.4$ kpc. This is similar to the weighted average $R_0 = 7.7 \pm 0.7$ kpc given by Reid (1989), which is based on four classes of determinations, namely (i) direct measurements, (ii) centroid of distributions, (iii) Galaxy models, and (iv) Eddington luminosity. Another similar result, $R_0 = 7.6 \pm 0.9$ kpc was obtained by Racine & Harris (1989) based on the fact that the space distribution of globular clusters around the galactic centre approximately follows an R^{-3} law.

3. Results and discussion

The gradients have been approximated both as a linear relationship of the form

$$\frac{d\log(\mathrm{X/H})}{dR} = a_1 + a_2 R \tag{1}$$

as in Maciel & Köppen (1994), and as a second order polynomial of the form

$$\frac{d\log(\mathrm{X/H})}{dR} = a_3 + a_4 R + a_5 R^2 \tag{2}$$

where R is in kpc. Fig. 1 shows the abundances and derived fits for the O/H, Ne/H, S/H and Ar/H ratios. The data points are shown, as well as the linear and second-order fits (solid lines). Alternatively, histograms of the PN abundances averaged in 1 kpc bins from $R =$ 3–4 kpc to $R = 13 - 14$ kpc are also shown. This procedure is probably more robust, as it washes out local discrepancies and uncertainties, and defines an average abundance at different galactocentric distances.

The derived coefficients $a_1 - a_5$ are given in Table 2, along with the number n of objects, the linear standard deviations $\sigma(a_1)$, $\sigma(a_2)$ and the correlation coefficient r.

[1] Available in electronic form at the CDS

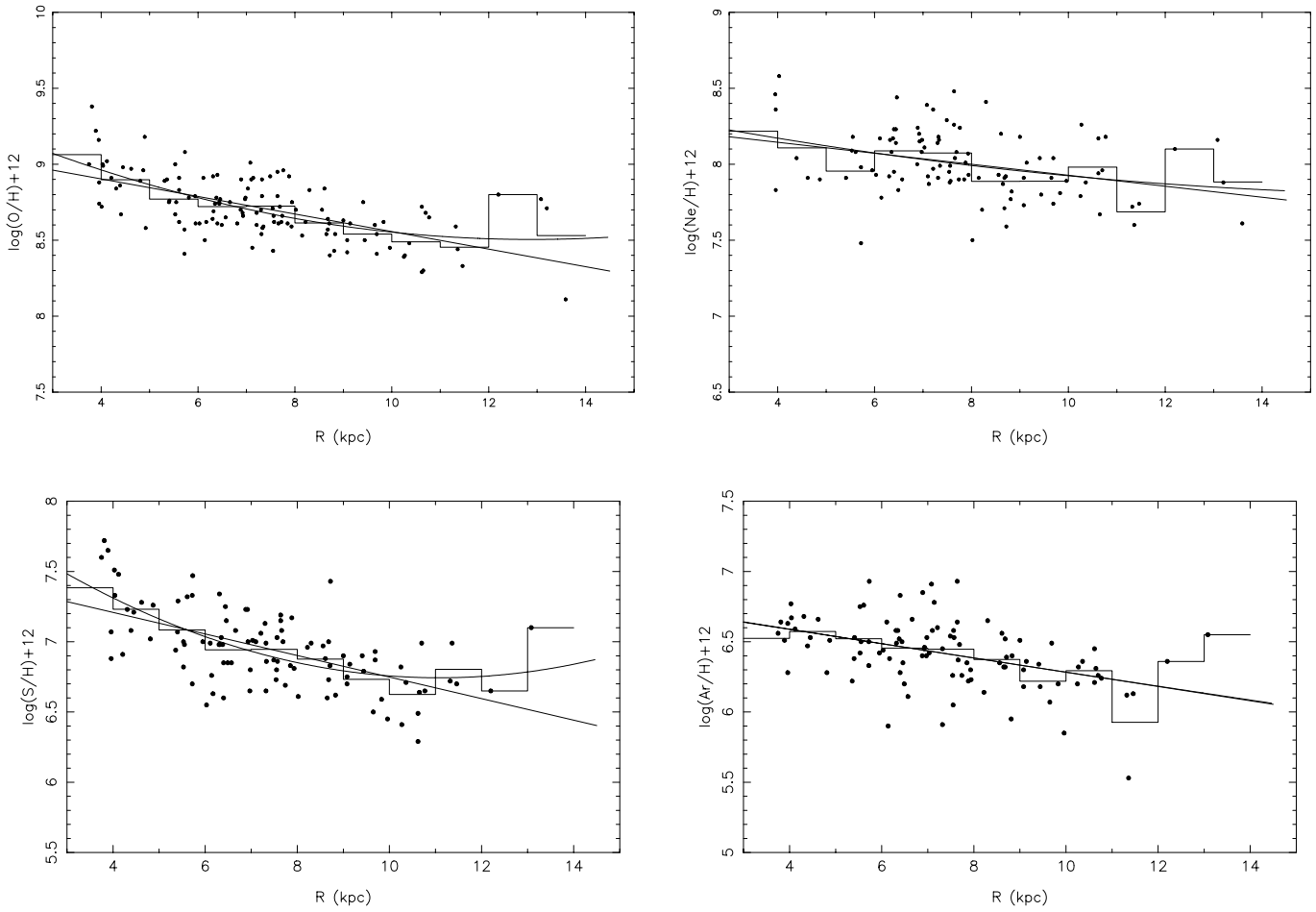

Fig. 1. Abundances and derived fits for PN. Solid lines: linear and second order polynomial fits; histograms: average abundances in 1 kpc bins.

Table 2. Coefficients of the linear and polynomial fits

	O/H	Ne/H	S/H	Ar/H
n	128	99	102	100
a_1	9.13	8.29	7.52	6.79
$\sigma(a_1)$	0.05	0.08	0.08	0.08
a_2	−0.058	−0.036	−0.077	−0.051
$\sigma(a_2)$	0.007	0.010	0.011	0.010
r	0.61	0.34	0.59	0.45
a_3	9.47	8.41	8.14	6.80
a_4	−0.149	−0.067	−0.251	−0.053
a_5	0.006	0.002	0.011	0.000

It can be seen that the main conclusions by Maciel and Köppen (1994) are maintained, in the sense that for $R \leq R_0$ a clear radial gradient can be observed for the O/H, Ne/H, S/H and Ar/H ratios, averaging $d\log(\mathrm{X/H})/dR \simeq -0.06$ dex/kpc, in excellent agreement with the well known O/H gradient of about -0.07 dex/kpc obtained from HII regions (Shaver et al. 1983, Edmunds 1992, Simpson et al. 1995). Moreover, the new results point to a flattening for galactocentric distances greater than R_0, particularly for $R \geq 10$ kpc. This is especially true for the O/H and S/H ratios, for which the polynomial fits are clearly distinguished from the linear fits. For Ne and Ar, some indication of flattening can also be seen, but the derived gradients are almost indistinguishable from a linear fit. In principle, this could mean that no flattening is present for these elements. However, the number of PN with reliable measurements of these elements is lower than for oxygen, and the associated uncertainties are greater, due to the faintness of the Ar lines (Costa et al. 1996). Also, the small number of PN near the extremes of Fig. 1, namely at $R \leq 4$ kpc and $R \geq 10$ kpc tends to flatten the gradients at the whole range of galactocentric distances, washing out part of the differences between the extremes. The fact that the inner gradients are steeper than the outer gradients is more clearly seen in the 1 kpc binned histograms also shown in Fig. 1. Near the anticentre direction the uncertainties increase due to the small number of data points, but the histograms definitely show some decrease in the slopes, even for Ne and Ar. The average uncertainties of the abundances of anticentre nebulae are similar to those of PN at $R < R_0$, provided the heliocentric distances are similar. Also, available data on the central stars does not indicate appreciable differences in the excitation conditions of the anticentre nebulae and those for which $R \leq R_0$, so that we believe the flattening shown in Fig. 1 to be real.

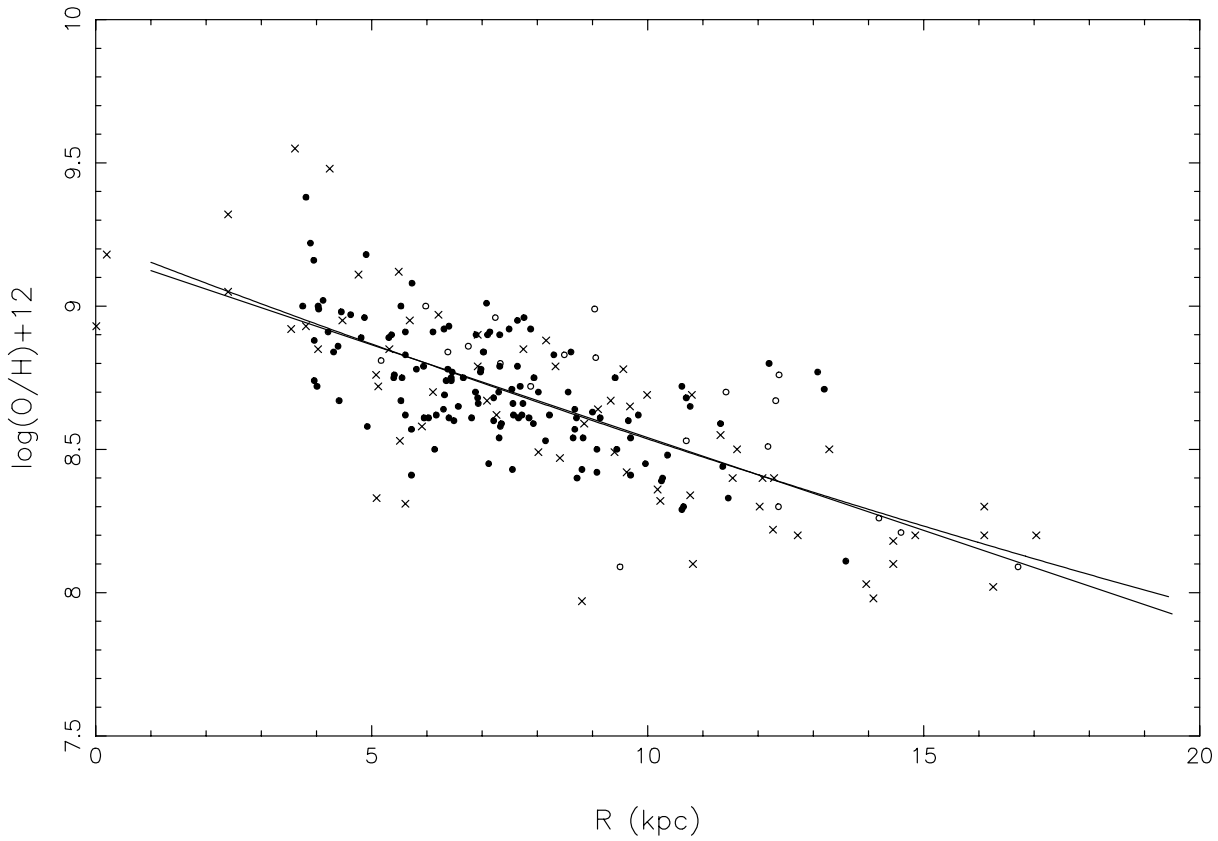

Fig. 2. O/H gradients for PN (filled circles), HII regions (crosses), and young stars (empty circles). The straight line represents an average gradient through all data of -0.065 dex/kpc.

The radial gradients as observed in the PN sample can be directly compared with the HII region data, correcting for $R_0 = 7.6$ kpc. Some recent discussions include Simpson et al. (1995), Esteban & Peimbert (1995), Vílchez & Esteban (1996), and Afflerbach et al. (1997), on the basis of radio, infrared and optical data. These authors give evidences for some flattening for galactocentric distances $R \geq 12$ kpc, in very good agreement with the results derived in this paper. On the other hand, Rudolph et al. (1997) derived an essentially constant slope for the S/H (and N/H) ratio in HII regions. However, their sample contains a very small number of objects at distances $R \geq 10$ kpc. If we consider their derived gradient as an average gradient for the solar region, their result is also in good agreement with the results presented here.

Regarding the stellar data, the analysis of abundance gradients becomes somewhat more complicated, as there are some inconsistencies in the results. Open cluster stars generally produce consistent results with HII regions (Janes 1995, Tosi 1995), as also cepheids and supergiants (Pagel 1992). On the other hand, data for Be stars seem to indicate an essentially flat gradient, as also happens with main sequence B stars (Fitzsimmons et al. 1990, Rolleston et al. 1993, Kaufer et al. 1994, Kilian-Montenbruck et al. 1994). However, recent work by Smartt & Rolleston (1997) eliminates some of these discrepancies, in the sense that a gradient has been obtained for an updated sample of B stars which is very similar to the HII region and PN gradient near the sun's position. As a general conclusion, these results support the results presented here regarding the magnitude of the gradient for galactocentric distances $R \leq R_0$. At the outer Galaxy, the situation is less clear. The flattening of the gradients is better observed in the PN data, as can be seen in Fig. 1 and also from Fig. 2 for O/H. In this figure, the crosses are HII regions from the sample considered by Allen et al. (1998), which comprises objects from Vílchez & Esteban (1996), Shaver et al. (1983) and Peimbert (1979). To these, HII regions from Rudolph et al. (1997) and Simpson et al. (1995) have also been added. Stellar data from Smartt and Rolleston (1997), which are basically B stars in young galactic open clusters are also shown (empty circles), apart from our own PN results (filled circles). The straight line shows an average linear gradient for all objects of about -0.065 dex/kpc. Some deviation from a second-order polynomial (solid curve) can also be seen, especially at large R. Taking the HII regions and B stars separately, a steeper gradient is obtained, ≤ -0.07 dex/kpc.

Within the uncertainties of the data, it seems that an average gradient of -0.04 to -0.07 dex/kpc can be derived for the inner Galaxy, a region loosely defined by $4 \leq R(\mathrm{kpc}) \leq 10$ for $R_0 = 7.6$ kpc. The gradients show a small variation for the different element ratios, and the PN gradients are generally slightly flatter than those derived from younger objects. For larger galactocentric distances, the PN gradients show some flattening in agreement with part of the stellar data, but it is possible that

no flattening exists for B stars (cf. Smartt & Rolleston 1997), which could be explained by the temporal variations of the gradients suggested by Maciel & Köppen (1994). The precise region where the gradient flattens out is not very well defined, due to the mentioned uncertainties, so that there is an intermediate region where the results are relatively inconclusive. This explains the fact that some of the Be stars at $R \leq 10$ kpc are apparently consistent with a flat gradient, as obtained by Rolleston et al. (1993). In fact, we need better abundances and especially a much larger sample of both young stars and photoionized nebulae to settle this question, particularly at $R \geq 12$ kpc.

Regarding the time variations of the gradients, analysis of the different objects included in Fig. 2 points to some interesting conclusions. Generally speaking, the PN gradients are flatter by about 0.01–0.03 dex/kpc than the corresponding gradients derived from the younger objects, suggesting some temporal steepening of the gradients, in agreement with the conclusions by Maciel & Köppen (1994). Also, the gradients derived from HII regions are slightly steeper than that for B stars, confirming the suggested tendency. It is difficult to assign precise ages for disk PN, but adopting the average values given by Maciel & Köppen (1994), $\tau \sim 5$ Gyr and $\Delta[d\log(\mathrm{O/H})/dR] \sim -0.02$ dex/kpc, we could obtain *a very rough idea* of the average steepening rate r for the galactic disk by

$$r \sim \frac{1}{\tau}\,\Delta\left[\frac{d\log(\mathrm{O/H})}{dR}\right] \sim -0.004\ \mathrm{dex\ kpc^{-1}\ Gyr^{-1}} \qquad (3)$$

where the minus sign emphasizes the fact that the gradients become progressively more negative with time. Assuming that this rate has remained constant for the whole lifetime of the Galaxy $\tau_G \sim 13$ Gyr, an initial gradient of about -0.02 dex/kpc would be obtained, that is, an essentially flat abundance distribution. It should be stressed that Eq. (3) is very approximate due to several reasons, such as the abundance uncertainties for PN, the inhomogeneity of the data, and the lack of reliable ages. However, the time evolution of the gradients affects chemical evolution models in a particularly striking way, so that it is interesting to explore some of the consequences of a larger albeit inhomogeneous sample of HII regions, PN and stars.

Recent chemical evolution models are generally able to explain the presence of abundance gradients, at least if these are considered as an average decrease of the abundances with increasing galactocentric distances. However, taking into account not only the *magnitude* of the gradients, but also their *space* and *temporal* variations, the number of models that are still able to explain the observed features decreases considerably. As an example, the recent multiphase models by Ferrini and collaborators (see for example Ferrini et al. 1992) predict some temporal flattening of the gradients, in contrast with the conclusions by Maciel and Köppen (1994) on the basis of disk PN. The predicted magnitudes of the gradients are similar, and even steeper than observed for these objects (Mollá et al. 1997, Mollá & Ferrini 1995). However, for large galactocentric distances, the models predict a *steepening* of the gradients, in contradiction with the results of the present work and from the analysis of HII regions in the outer Galaxy. Similar results have also been obtained by the recent models of Allen et al. (1998).

Classical chemical evolution models along the lines of the models by Matteucci & François (1989) have been recently developed (Chiappini et al. 1997), and predict generally flatter gradients than observed. On the other hand, these models are consistent with some steepening in the inner Galaxy and a corresponding flattening near the outer parts, in agreement with the results presented in this paper. These models predict some temporal steepening of the gradients, which is also supported by the present results and those by Maciel & Köppen (1994).

Perhaps the most promising theoretical models are the so-called chemodynamical models, as discussed for example by Burkert & Hensler (1987, 1988). Recent results applied to disk galaxies (Samland & Hensler 1996, Samland et al. 1997, Hensler 1999) are in a good agreement with the gradients from photoionized nebulae, both regarding the magnitude of the gradients and their space variations. Since the application of this kind of model to galaxies like our own is still in its infancy, it is expected that more detailed models will be able to account also for the time behaviour of the abundance variations in the near future.

Acknowledgements. This work was partially supported by FAPESP and CNPq.

References

Acker A., Ochsenbein F., Stenholm B., et al., 1992, Strasbourg-ESO Catalogue of Galactic Planetary Nebulae. ESO
Allen C., Carigi L., Peimbert M., 1998, ApJ 494, 247
Afflerbach A., Churchwell E., Werner M.W., 1997, ApJ 478, 190
Amnuel P.R., 1993, MNRAS 261, 263
Amnuel P.R., Guseinov O.H., Novruzova H.I., Rustamov Yu., 1984, Ap&SS 107, 19
Burkert A., Hensler G., 1987, MNRAS 225, 21P
Burkert A., Hensler G., 1988, MNRAS 199, 131
Cahn J.H., Kaler J.B., Stanghellini L., 1992, ApJS 94, 399
Cazetta J.O., Maciel W.J., 1994, A&A 290, 936
Chiappini C., Matteucci F., Gratton R., 1997, ApJ 477, 765
Corradi R.L.M., Perinotto M., Schwarz H.E., Claeskens J.F., 1997, A&A 322, 975
Costa R.D.D., Chiappini C., Maciel W.J., Freitas Pacheco J.A., 1996, A&AS 116, 249
Costa R.D.D., Chiappini C., Maciel W.J., Freitas Pacheco J.A., 1997, In: Rood R.T., Renzini A. (eds.) Advances in stellar evolution. CUP, Cambridge, 159
D'Odorico S., Peimbert M., Sabbadin F., 1976, A&A 47, 341
Edmunds M.G., 1992, In: Edmunds M.G., Terlevich R.J. (eds.) Elements and the cosmos. CUP, Cambridge, 289
Esteban C., Peimbert M., 1995, Rev. Mex. Astron. Astrof. SC 3, 133
Faúndez-Abans M., Maciel W.J., 1986, A&A 158, 228
Faúndez-Abans M., Maciel W.J., 1987, A&A 183, 324
Ferguson A.M.N., Gallagher J.S., Wyse R.F.G., 1998, AJ 116, 673
Ferrini F., Matteucci F., Pardi C., Penco U., 1992, ApJ 387, 138
Fitzsimmons A., Brown P.T.F., Dufton P.L., Lennon D.J., 1990, A&A 232, 437
Hajian A.R., Balick B., Terzian Y., Perinotto M., 1997, ApJ 487, 313
Hensler G., 1999, In: Spite M., Spite F. (eds.) Galaxy evolution. In press

Henry R.B.C., Howard J.W., 1995, ApJ 438, 170
Janes K., 1995, In: Alfaro A., Delgado A.J. (eds.) The formation of the Milky Way. CUP, Cambridge, 144
Kaufer A., Szeifert T., Krenzin R., Baschek B., 1994, A&A 289, 740
Kennicutt R.C., Garnett D.R., 1996, ApJ 456, 504
Kilian-Montenbruck J., Gehren T., Nissen P.E., 1994, A&A 291, 757
Kingsburgh R.L., Barlow M.J., 1994, MNRAS 271, 257
Köppen J., Acker A., Stenholm B., 1991, A&A 248, 208
Maciel W.J., 1984, A&AS 55, 253
Maciel W.J., 1992, In: Edmunds M.G., Terlevich R.J. (eds.) Elements and the cosmos. CUP, Cambridge, 210
Maciel W.J., 1993, Ap&SS 206, 285
Maciel W.J., 1997, In: IAU Symp. 180, Habing H.J., Lamers H.J.G.L.M. (eds.) Kluwer, Dordrecht, 397
Maciel W.J., Cazetta J.O., 1997, Ap&SS 249, 341
Maciel W.J., Chiappini C., 1994, Ap&SS 219, 231
Maciel W.J., Dutra C.M., 1992, A&A 262, 271
Maciel W.J., Köppen J., 1994, A&A 282, 436
Matteucci F., François P., 1989, MNRAS 239, 885
Mollá M., Ferrini F., 1995, ApJ 454, 726
Mollá M., Ferrini F., Díaz A.I., 1997, ApJ 475, 519
Pagel B.E.J., 1992, In: Barbuy B., Renzini A. (eds.) IAU Symp. 149, Kluwer, Dordrecht, 133
Pasquali A., Perinotto M., 1993, A&A 280, 581
Peimbert M., 1978, In: Terzian Y. (ed.) IAU Symp. 76, Reidel, Dordrecht, 215
Peimbert M., 1979, In: Burton W.B. (ed.) IAU Symp. 84, Reidel, Dordrecht, 307
Peimbert M., 1990, Rep. Prog. Phys. 53, 1559
Peimbert M., Torres-Peimbert S., 1983, In: Flower D.R. (ed.) IAU Symp. 103, Reidel, Dordrecht, 233
Peimbert M., Carigi L., 1998, In: Friedli D., Edmunds M.G., Robert C., Drissen L. (eds.) ASP Conf. Ser. 147, 88
Perinotto M., 1991, ApJS 76, 687
Perinotto M., Purgathofer A., Pasquali A., Patriarchi P., 1994, A&AS 107, 495
Racine R., Harris W.E., 1989, AJ 98, 1609
Reid M.J., 1989, In: Morris M. (ed.) The center of the Galaxy. Reidel, Dordrecht, p. 37
Rolleston W.R.J., Brown P.J.F., Dufton P.L., Fitzsimmons A., 1993, A&A 270, 107
Rudolph A.L., Simpson J.P., Haas M.R., Erickson E.F., Fich M., 1997, ApJ 489, 94
Samland M., Hensler G., 1996, In: Blitz L., Teuben P. (eds.) IAU Symp. 169, Kluwer, Dordrecht, 395
Samland M., Hensler G., Theis C., 1997, ApJ 476, 544
Samland M., Köppen J., Acker A., Stenholm B., 1992, A&A 264, 184
Shaver P.A., McGee R.X., Newton L.M., Danks A.C., Pottasch S.R., 1983, MNRAS 204, 53
Simpson J.P., Colgan S.W.J., Rubin R.H., Erickson E.F., Haas M.R., 1995, ApJ 444, 721
Smartt S.J., Rolleston W.R.J., 1997, ApJ 481, L47
Terzian Y., 1993, In: Weinberger R., Acker A. (eds.) IAU Symp. 155, Kluwer, Dordrecht, 109
Terzian Y., 1997, In: Habing H.J., Lamers H.J.G.L.M. (eds.) IAU Symp. 180, Kluwer, Dordrecht, 29
Tosi M., 1995, In: Alfaro A., Delgado A.J. (eds.) The formation of the Milky Way. CUP, Cambridge, 153
Villa-Costas M.B., Edmunds M.G., 1992, MNRAS 259, 121
Vílchez J.M., Esteban C., 1996, MNRAS 280, 720
Vílchez J.M., Pagel B.E.J., Díaz A.I., Terlevich E., Edmunds M.G., 1988, MNRAS 235, 633
Zaritsky D., Kennicutt R.C., Huchra J.P., 1994, ApJ 420, 87

Table 1 - Data for disk planetary nebulae

name	PNG	d	R	ϵ(O)	ϵ(Ne)	ϵ(S)	ϵ(Ar)	Ref.
NGC 40	120.0+09.8	0.8	8.02	8.70	7.50	6.61	0.00	1
NGC 1535	206.4−40.5	1.6	8.71	8.61	7.92	6.83	6.39	1
NGC 2022	196.6−10.9	2.2	9.69	8.41	8.04	6.93	6.49	1
NGC 2371	189.1+19.8	1.5	9.00	8.63	8.18	6.90	6.51	1
NGC 2392	197.8+17.3	2.0	9.44	8.50	7.80	6.79	6.18	1
NGC 2438	231.8+04.1	1.5	8.61	8.84	8.20	6.88	6.56	1
NGC 2452	243.3−01.0	2.7	9.14	8.61	8.01	6.84	6.36	6
NGC 2792	265.7+04.1	1.8	7.94	8.75	7.93	0.00	6.23	1
NGC 2867	278.1−05.9	1.6	7.54	8.71	7.95	6.73	6.26	1
NGC 3132	272.1+12.3	1.1	7.64	8.95	8.48	7.19	6.93	1,2
NGC 3195	296.6−20.0	2.4	6.89	8.90	8.24	0.00	6.85	1
NGC 3211	286.3−04.8	2.5	7.30	8.70	8.14	7.13	0.00	1
NGC 3242	261.0+32.0	0.8	7.74	8.66	7.90	6.69	6.26	1
NGC 3587	148.4+57.0	0.7	7.93	8.59	8.07	6.81	6.30	1
NGC 3699	292.6+01.2	2.0	7.08	9.01	8.39	0.00	6.91	2
NGC 3918	294.6+04.7	2.2	6.98	8.78	8.16	6.80	6.53	1
NGC 5307	312.3+10.5	2.3	6.30	8.64	7.92	6.98	0.00	1
NGC 5882	327.8+10.0	1.6	6.32	8.69	8.16	6.98	6.49	1
NGC 6210	043.1+37.7	1.3	6.88	8.70	8.00	7.23	6.40	1
NGC 6309	009.6+14.8	2.1	5.61	8.91	8.08	7.32	6.76	1
NGC 6439	011.0+05.8	3.8	3.96	8.88	8.36	7.07	6.63	1
NGC 6543	096.4+29.9	0.7	7.69	8.72	8.08	7.00	6.48	1
NGC 6563	358.5−07.3	1.9	5.72	8.57	7.98	7.33	6.33	1
NGC 6565	003.5−04.6	1.5	6.11	8.91	8.17	6.99	6.64	1
NGC 6567	011.7−00.6	1.5	6.14	8.50	7.78	6.76	5.90	1
NGC 6572	034.6+11.8	0.8	6.97	8.77	8.08	6.65	6.40	1
NGC 6578	010.8−01.8	2.1	5.55	8.75	8.18	6.98	6.50	1
NGC 6629	009.4−05.0	1.6	6.03	8.61	7.93	6.55	6.44	1
NGC 6720	063.1+13.9	0.7	7.32	8.79	8.18	6.99	6.45	1
NGC 6790	037.8−06.3	1.5	6.49	8.60	7.83	6.85	6.20	1

Table 1 - continued

name	PNG	d	R	ϵ(O)	ϵ(Ne)	ϵ(S)	ϵ(Ar)	Ref.
NGC 6818	025.8−17.9	1.5	6.35	8.74	8.08	7.03	6.58	1
NGC 6826	083.5+12.7	0.7	7.55	8.43	7.88	6.80	6.05	1
NGC 6879	057.2−08.9	3.7	6.40	8.61	7.95	6.60	6.28	1
NGC 6884	082.1+07.0	1.7	7.56	8.66	7.99	7.03	6.58	1
NGC 6886	060.1−07.7	1.7	6.92	8.68	8.20	7.23	6.45	1
NGC 6891	054.1−12.1	2.2	6.57	8.65	7.90	6.85	6.11	1
NGC 6894	069.4−02.6	1.5	7.21	8.60	7.97	0.00	0.00	1
NGC 6905	061.4−09.5	1.8	6.93	8.66	8.15	7.00	6.46	1
NGC 7009	037.7−34.5	0.9	7.03	8.84	8.11	7.01	6.42	1
NGC 7026	089.0+00.3	0.9	7.64	8.79	8.26	7.15	6.64	1
NGC 7027	084.9−03.4	0.7	7.57	8.62	7.89	6.86	6.53	1
NGC 7354	107.8+02.3	0.8	7.88	8.92	8.01	7.17	6.22	5
NGC 7662	106.5−17.6	0.8	7.85	8.61	7.90	6.83	6.35	1
IC 351	159.0−15.1	3.0	10.36	8.48	7.88	6.71	6.36	1
IC 418	215.2−24.2	1.6	8.83	8.54	7.82	6.62	6.40	1
IC 1297	358.3−21.6	3.0	4.81	8.89	0.00	7.02	6.28	1
IC 1747	130.2+01.3	2.5	9.41	8.75	8.04	6.90	6.34	1
IC 2003	161.2−14.8	2.4	9.83	8.62	7.81	6.59	6.20	1
IC 2149	166.1+10.4	1.1	8.65	8.54	7.87	6.60	6.32	1
IC 2165	221.3−12.3	1.9	9.08	8.42	7.91	6.75	6.30	1
IC 2448	285.7−14.9	2.9	7.35	8.59	7.99	0.00	0.00	1
IC 2501	281.0−05.6	0.8	7.49	8.92	8.29	6.87	6.54	1
IC 2621	291.6−04.8	2.1	7.10	8.90	7.92	7.00	6.58	1
IC 3568	123.6+34.5	2.1	8.68	8.57	7.91	7.00	6.52	1
IC 4406	319.6+15.7	1.7	6.44	8.75	8.23	7.25	6.50	2,4,7
IC 4776	002.0−13.4	3.3	4.39	8.86	8.04	7.08	6.47	1
IC 5117	089.8−05.1	1.0	7.66	8.61	8.04	7.08	6.37	1
IC 5217	100.6−05.4	2.8	8.56	8.70	7.93	6.97	6.35	1
BD+303639	064.7+05.0	0.7	7.33	8.58	8.16	6.86	0.00	1
Cn2-1	356.2−04.4	3.6	4.03	9.00	8.58	7.51	6.77	1

Table 1 - continued

name	PNG	d	R	ϵ(O)	ϵ(Ne)	ϵ(S)	ϵ(Ar)	Ref.
Fg 1	290.5+07.9	2.4	7.12	8.45	7.87	0.00	0.00	1
H1-13	352.8−00.2	0.8	6.81	8.61	0.00	0.00	0.00	7
H1-17	358.3+03.0	3.8	3.81	9.38	0.00	7.72	6.64	9
H1-32	355.6−02.7	2.7	4.92	8.58	0.00	0.00	0.00	8
H1-44	358.9−03.7	3.2	4.41	8.67	0.00	0.00	0.00	8
H1-56	001.7−04.6	3.6	4.01	8.72	0.00	0.00	0.00	8
H2-37	002.3−03.4	2.0	5.61	8.62	0.00	0.00	0.00	8
Hb 4	003.1+02.9	2.2	5.41	8.76	7.91	7.29	6.53	1,5
Hb 5	359.3−00.9	1.2	6.40	8.93	8.23	6.85	6.83	1
Hb 12	111.8−02.8	2.3	8.72	8.40	7.59	7.43	0.00	1
He2-21	275.3−04.7	7.2	9.96	8.45	7.89	6.45	5.85	2
He2-29	275.8−02.9	4.0	8.22	8.62	7.70	6.96	6.14	6
He2-37	274.6+03.5	2.3	7.76	8.96	8.24	0.00	0.00	1
He2-47	285.6−02.7	2.0	7.32	8.90	0.00	6.65	5.91	7,9
He2-48	282.9+03.8	5.1	8.15	8.53	7.91	0.00	0.00	1
He2-51	288.8−05.2	3.0	7.21	8.68	8.36	7.06	6.60	1,6,7
He2-55	286.3+02.8	2.6	7.31	8.54	7.91	0.00	0.00	1
He2-67	292.8+01.1	4.3	7.14	8.91	0.00	0.00	6.78	7
He2-86	300.7−02.0	2.6	6.66	8.75	0.00	7.08	6.66	1
He2-99	309.0−04.2	4.2	5.94	8.79	0.00	0.00	0.00	1
He2-112	319.2+06.8	2.5	5.95	8.61	7.96	7.00	6.42	1,6
He2-115	321.3+02.8	2.0	6.17	8.62	0.00	6.63	6.38	1
He2-118	327.5+13.3	8.4	4.45	8.98	0.00	7.21	6.53	9
He2-119	317.1−05.7	1.7	6.46	8.77	8.44	7.15	6.35	1,6,7
He2-123	323.9+02.4	2.9	5.53	8.67	0.00	6.82	6.42	1
He2-138	320.1−09.6	3.1	5.61	8.83	0.00	0.00	0.00	1
He2-140	327.1−01.8	2.9	5.40	8.75	0.00	7.07	6.38	1
He2-141	325.4−04.0	2.8	5.53	9.00	8.09	7.00	6.75	2
He2-157	331.0−02.7	5.4	3.89	9.22	0.00	7.65	6.51	1
He2-158	327.8−06.1	10.0	5.36	8.90	0.00	6.94	6.22	1

Table 1 - continued

name	PNG	d	R	ϵ(O)	ϵ(Ne)	ϵ(S)	ϵ(Ar)	Ref.
He2-250	000.7+03.2	2.7	4.90	9.18	0.00	0.00	0.00	8
Hu1-1	119.6−06.7	4.7	10.70	8.68	7.96	6.99	6.26	1
J 320	190.3−17.7	4.1	11.46	8.33	7.74	6.70	6.13	1
J 900	194.2+02.5	2.1	9.65	8.60	7.91	6.50	6.07	1
K1-7	197.2−14.2	5.8	13.08	8.77	8.16	7.10	6.55	3
K3-66	167.4−09.1	6.7	14.13	7.89	0.00	5.91	5.90	3
K3-68	178.3−02.5	6.0	13.59	8.11	7.61	0.00	0.00	8
M1-1	130.3−11.7	4.1	10.65	8.30	7.67	6.64	6.31	1
M1-4	147.4−02.3	1.7	9.08	8.50	7.73	6.70	6.18	1
M1-5	184.0−02.1	2.1	9.69	8.54	7.74	6.87	0.00	1
M1-7	189.8+07.7	5.7	13.20	8.71	7.88	0.00	0.00	8
M1-8	210.3+01.9	3.5	10.77	8.65	8.18	6.65	6.24	6
M1-11	232.8−04.7	2.1	9.02	7.88	0.00	5.82	5.28	3
M1-14	234.9−01.4	3.8	10.27	8.40	8.26	6.41	6.32	3
M1-17	228.8+05.3	5.8	12.20	8.80	8.10	6.65	6.36	8
M1-25	004.9+04.9	3.6	4.04	8.99	0.00	7.33	6.67	1
M1-34	357.9−05.1	3.5	4.12	9.02	0.00	7.48	6.59	1
M1-38	002.4−03.7	3.4	4.21	8.91	0.00	6.91	0.00	1
M1-40	008.3−01.1	1.9	5.73	9.08	0.00	7.47	6.93	1,9
M1-50	014.6−04.3	3.9	3.96	8.74	7.83	6.88	6.28	1
M1-54	016.0−04.3	3.2	4.62	8.97	7.91	7.28	6.66	1
M1-57	022.1−02.4	3.1	4.87	8.96	7.90	7.26	6.51	1
M1-60	019.7−04.5	3.7	4.31	8.84	0.00	7.23	6.68	9
M1-74	052.2−04.0	2.5	6.38	8.78	8.17	6.98	6.52	1
M1-79	093.3−02.4	1.0	7.72	8.62	0.00	0.00	0.00	8
M1-80	107.7−02.2	6.4	11.32	8.59	7.72	6.72	6.12	1
M2-2	147.8+04.1	1.4	8.81	8.43	7.77	0.00	5.95	1
M2-10	354.2+04.3	3.9	3.75	9.00	0.00	7.60	6.56	1
M2-16	357.4−03.2	1.8	5.81	8.78	0.00	0.00	0.00	8
M2-27	359.9−04.5	2.3	5.31	8.89	0.00	0.00	0.00	8

Table 1 - continued

name	PNG	d	R	ϵ(O)	ϵ(Ne)	ϵ(S)	ϵ(Ar)	Ref.
M3-1	242.6−11.6	4.3	10.25	8.39	7.79	6.82	6.20	6
M3-4	241.0+02.3	4.6	10.62	8.72	8.17	6.49	6.45	6
M3-5	245.4+01.6	4.9	10.62	8.29	7.94	6.29	6.21	6
M3-6	253.9+05.7	2.6	8.68	8.64	7.71	6.73	6.32	1
M3-15	006.8+04.1	1.9	5.72	8.41	7.48	6.70	6.50	1
MaC 2-1	205.8−26.7	4.5	11.36	8.44	7.60	6.99	5.53	3
PB 3	269.0−03.0	3.2	8.30	8.83	8.41	6.99	6.65	2
PC 14	336.2−06.9	4.5	3.95	9.16	8.46	0.00	0.00	1
Pe1-18	027.3−02.1	1.5	6.31	8.92	0.00	7.34	6.58	1
Th2-A	306.4−00.6	2.5	6.44	8.74	8.14	0.00	0.00	1

REFERENCES

1 - Maciel and Köppen (1994)

2 - Costa et al. (1996)

3 - Costa et al. (1997)

4 - Corradi et al. (1997)

5 - Hajian et al. (1997)

6 - Kingsburgh and Barlow (1994)

7 - Perinotto et al. (1994)

8 - Perinotto (1991)

9 - Köppen et al. (1991)